Full Length Article

Pulse electrodeposition of CoFe thin films covered with layered double hydroxides as a fast route to prepare enhanced catalysts for oxygen evolution reaction

Alan M.P. Sakita [a,b], Rodrigo Della Noce [c], Elisa Vallés [b,d], Assis V. Benedetti [a,*]

[a] Instituto de Química, UNESP-Universidade Estadual Paulista, 14800-900 Araraquara, Brazil
[b] Ge-CPN (Thin Films and Nanostructures Electrodeposition Group), Dpt. Ciència de Materials i Química Física, Martí i Franquès 1, 08028 Barcelona, Spain
[c] Centro de Química Estrutural-CQE, Departament of Chemical Engineering, Instituto Superior Técnico, Universidade de Lisboa, 1049-001 Lisboa, Portugal
[d] Institute of Nanoscience and Nanotechnology (IN2UB), Universitat de Barcelona, Spain

ARTICLE INFO

ABSTRACT

A novel, ultra-fast, and one-step method for obtaining an effective catalyst for oxygen evolution reaction is proposed. The procedure consists in direct electrodeposition, in a free-nitrate bath, of CoFe alloy films covered with layered double hydroxides (LDH), by potentiostatic mode, in continuous or pulsed regime. The catalyst is directly formed on glassy carbon substrates. The best-prepared catalyst material reveals a mixed morphology with granular and dendritic CoFe alloy covered with a sponge of CoFe-LDH containing a Cl interlayer. An overpotential of $\eta 10\,mA = 286\,mV$, with a Tafel slope of $48\,mV\,dec^{-1}$, is obtained for the OER which displays the enhanced properties of the catalyst. These improved results demonstrate the competitiveness and efficacy of our proposal for the production of OER catalysts.

© 2017 Elsevier B.V. All rights reserved.

1. Introduction

Water electrolysis reaction ($H_2O \rightarrow H_2 + 1/2O_2$), also called water splitting (WS), has attracted a great interest in last years mainly because it can be used for large-scale energy storage by using renewable energy sources [1,2]. However, one of the reactions involved in WS, the oxygen evolution reaction (OER), shows a low kinetics attributed to a four-electron multi-step reaction ($4OH^- \rightarrow 2H_2O + O_2 + 4e^-$, in alkaline medium) [3]. The OER can be enhanced by using catalysts that not only accelerate the reaction, but also decrease its overpotential. Oxides of noble metals such as IrO_2 and RuO_2 have shown good performance as electrocatalysts for water oxidation, inducing low overpotential and fast kinetics, which are attributed to the different oxidation states of Iridium and Ruthenium oxides and to the exchange between the different oxidation states during the reaction [4]. Nevertheless the high cost of the precursor metallic salts to prepare these catalysts, their low abundance, and the difficult extraction and manufacture of these metals are some drawbacks that limit their use for OER.

Therefore, much effort has been done to lower the production colour costs of OER catalysts, especially for obtaining (oxy)hydroxides and layered double hydroxides (LDHs) of earth-abundance and cost-effective transition metals [5]. The catalytic properties of these earth-abundant metal oxides/hydroxides are related to their ability to exchange oxidation states, e.g. Ir and Ru oxides, which make them potential materials for WS applications [6,7].

Among the preparation methods of oxides/hydroxides of transition metals with enhanced electrochemical properties for OER, the solvothermal [2,8] and hydrothermal [9,10] synthesis have shown to be reasonable methods for the preparation of catalysts with low overpotential for the WS reaction. Their high cost of production due to the time-consuming of synthesis and the need of using high temperature and pressure are obstacles that hinder their widespread utilization, however. Additionally, their large-scale production implies a solvent separation step, which requires the utilization of centrifuges and filtering systems that makes the process costly.

Electrodeposition may be used for the preparation of (oxy)hydroxides of transition metals directly over the substrate due to its benefits such as low cost and no need of binders [11,12]. Typically, researchers have tested this possibility by electrodepositing the metal (oxy)hydroxides using nitrate-containing

---

* Corresponding author.
  E-mail addresses: benedeti@iq.unesp.br, avbenedetti@gmail.com (A.V. Benedetti).

medium because the cathodically induced nitrate reduction ($NO_3^- + 7H_2O + 8e^- \rightarrow NH_4^+ + 10OH^-$) produces significant amount of OH^- ions that react with metal ions to form hydroxides on the substrate surface [12,13]. In this work, we propose a novel, facile, fast, nitrate-free, and one-step synthesis to directly obtain CoFe thin films covered by layered double hydroxides (CoFe//LDH) with enhanced catalytic electrochemical properties for water splitting. Moreover, catalysts obtained by means of pulse electrodeposition are optimized and compared with those obtained by continuous potential application.

2. Experimental section

2.1. Deposition solution

The deposition solution was prepared by dissolving the metal chloride salts (FeCl$_2$·4H$_2$O Sigma-Aldrich 99.0% and CoCl$_2$·6H$_2$O Panreac Analytical Grade) in Milli-Q quality water to reach 0.1 M of each metallic salt, and 0.5 M KCl as supporting electrolyte. Oxygen was removed from the solution using argon during 20 min to avoid the Fe^{2+} ion oxidation. The solution pH was about 2.5–3, and did not change by the addition of dilute acids or bases.

2.2. Electrodeposition process

The deposition of CoFe//LDH was performed on glassy carbon (GC) electrodes with geometric area of 0.071 cm^2, using potentiostatic method. GC electrode was polished to mirror-like finishing with alumina slurry of 0.3 μm. The potentials were applied for 5 s for all the deposited materials. Other tests were performed by applying potentials from 1 to 60 s but the optimum condition in terms of catalytic activity was obtained for the deposits prepared at 5 s, both in continuous and in pulse regimes. The pulsed deposition was performed with equal t_{on} and t_{off}, with a total time of t_{on} = 5 s. The scheme 1 (Supplementary material) shows the described process for pulsed deposition. For the electrodeposition process, Ag|AgCl|KCl$_{3M}$ reference electrode was used while the counter electrode was a Ti/Rh spiral. All the potentials of the deposition process are referred to this reference electrode.

2.3. Electrochemical studies

The electrochemical studies were performed using a microcomputer-controlled potentiostat/galvanostat AUTOLAB PGSTAT30 and GPES software. For the water splitting experiments, the reference electrode was a reversible hydrogen electrode (RHE) and a Ti/Rh wire was employed as counter electrode. The water splitting experiments were carried out using a 1 M NaOH solution and the polarization curves were obtained at 5 mV s^{-1}. The voltammetric curves showed in this work have no IR correction.

2.4. Surface characterization

XPS (X-ray photoelectron spectroscopy) experiments were conducted in a PHI 5500 Multitechnique System (from Physical Electronics) with a monochromatic X-ray source.

X ray diffraction (XRD) experiments were registered in a PANalytical X'Pert PRO MPD powder diffractometer Bragg-Brentano geometry and θ/θ goniometer. Nickel filtered Cu Kα radiation (λ = 1.5418 Å) and a work power of 45 kV–40 mA were used.

Raman spectroscopy was performed using a Jobin Yvon-Horiba LabRam HR800 equipment and the 532 nm green excitation wavelength from a Nd:YAG laser.

FE-SEM (Field emission scanning electron microscopy) analysis was performed using a JEOL J-7100 operating with electron acceleration of 2 keV.

3. Results and discussion

A voltammetric study of the CoFe deposition process on glassy carbon substrates was performed to select the best conditions for the preparation of CoFe//LDH catalysts. Potentials sufficiently negative to induce H$_2$ evolution, with consequent increase of the local pH, were selected to prepare the oxidized catalysts. The aim was to obtain deposits composed of CoFe alloy directly covered with LDH. Fig. SM1 shows the cyclic voltammograms of the solution containing Fe(II) and Co(II), at different scan rates, from which the onset of the deposition process was detected at about −1.0 V at 10 mV s^{-1}. After that, a diffusion-controlled peak for the reduction of Co(II) and Fe(II) was observed at –1.12 V. The scan to more negative potentials shows a fast increase of the cathodic current at −1.25 V, related to the hydrogen evolution reaction (HER). From this study, we tested deposition potentials in the −1.0 to −1.8 V range, selecting values ca. −1.4 V as the more adequate to avoid pure CoFe alloy deposition and excessive hydroxides formation. Short deposition times were used in order to obtain thin particulate deposits with a high area/volume ratio and adherent to the glassy carbon substrate.

Figs. 1 and SM2 show the SEM images of deposits obtained in continuous at −1.4 V and pulse deposition with different t_{on}. For all samples, at least three different structures can be observed: a granular underlayer mainly composed of nanograins, most likely, of CoFe alloy, a second layer related to metallic oxides, and a pine-like CoFe alloy top layer. The pulsed deposits obtained with 1 s ≤ t_{on} ≤ 0.5 s (Figs. 1B and C and SM2B and C) present less metal underlayer, more homogeneous and spongious layer of oxides, and low proportion of dendritic structures, due to the recovery of the metallic ion concentration near the electrode surface caused by the t_{off} step. However, when t_{on} decreases to <0.5 s, alloy dendrites increase again, because the t_{off} time is not enough to recover the surface concentration. The three types of structures observed in the deposits (granular, oxide interlayer and dendritic) can be justified by the shape of the chronoamperometric curves recorded during the material deposition. For the continuous deposition (Fig. 2), at the initial times, an increase of current density, typical of a nucleation process, is observed, which corresponds to the formation of CoFe nuclei. Subsequently, the contribution of a new current (observed in Fig. 2 at potentials of −1.4 and −1.8 V) referred to HER over the initial deposit appears [14,15]. This simultaneous reaction drastically consumes the H$^+$ near the electrode surface, increasing the local pH and favoring the instantaneous hydroxides formation [16,17]. Moreover, the more superficial pine-like structure, e.g. dendritic growth, might be a consequence of the simultaneous alloy formation and hydrogen evolution during the electrodeposition process [18].

In the pulsed deposition (Fig. 2B) the current corresponding to HER decreases as the t_{on} also diminishes, although the formation of CoFe alloy catalyzes the HER and always induces the formation of the oxide layer. However, when the pulses are very short, the deposits are mainly composed of the alloy. Therefore, the more adequate deposits as OER catalysts will be, probably, those obtained by means of pulsed deposition with t_{on} values in the range 0.5 to 1 s, which present the higher proportion of the oxide layer. The morphology of the deposits is similar to that obtained by Burke et al. [19] for CoFe//LDH, where LDH represents a Layered Double Hydroxide structure, but in our work the simultaneous H$^+$ electroreduction and local pH increase directly induce the formation of oxidized species.

The XRD patterns of representative deposits obtained at −1.4 V show very small peaks over the signal of the GC substrate (Fig. 3A). In order to clearly detect the structure of the deposits, several replicate deposits were obtained on GC and accumulated on a silicon holder; Fig. 3B shows now very visible peaks corresponding to crystalline phases in the deposits: the peaks (marked in red in
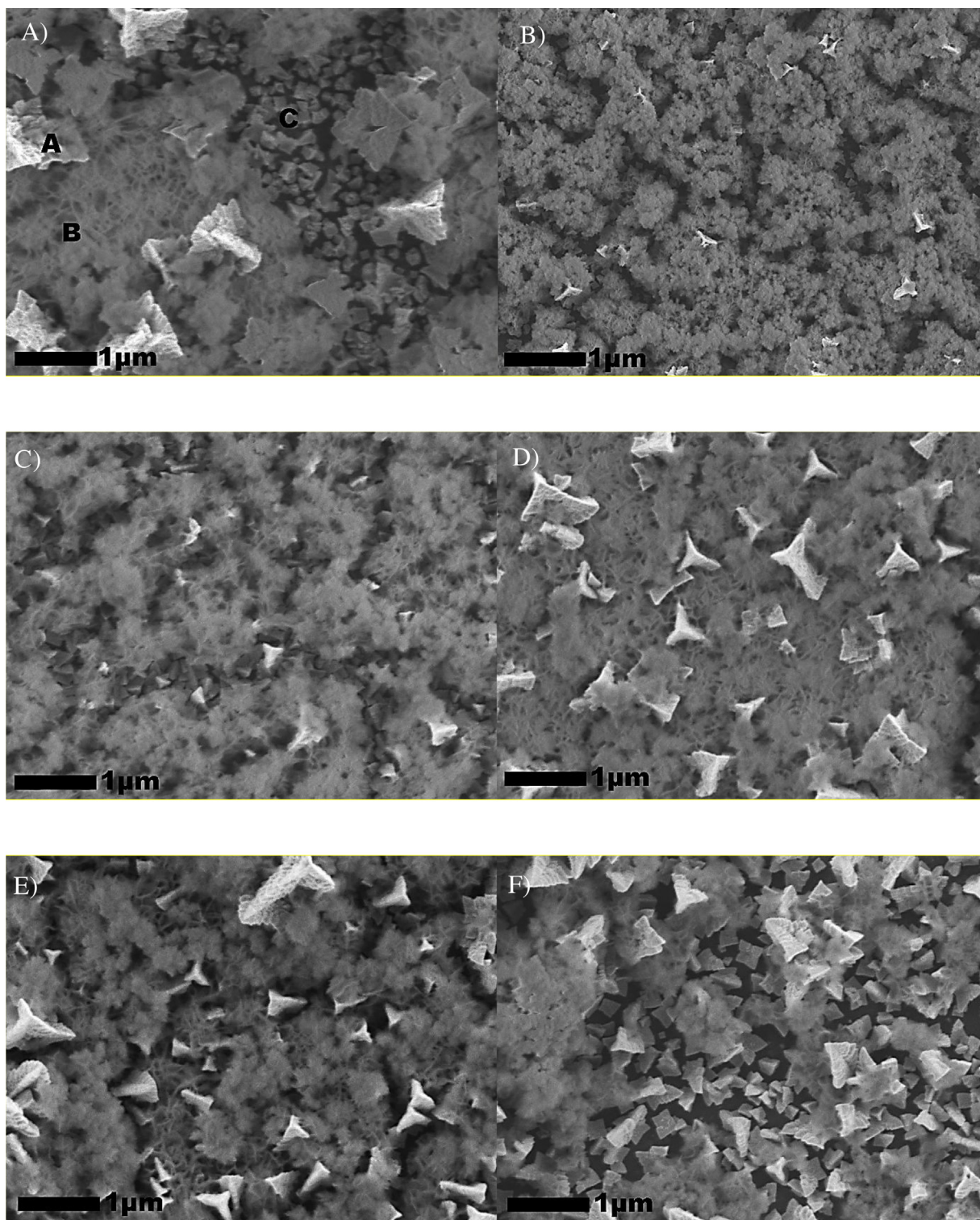
Fig. 1. FE-SEM images of deposit obtained on GC at −1.4 V/Ag|AgCl|KCl$_{3M}$ A) constant potential during 5 s: insert (A) top-layer; (B) intermediate layer; (C) underlayer. B to F) pulse deposition with 5 pulses of t$_{on}$ = t$_{off}$ of B) 1 s, C) 0.5 s, D) 0.25 s, E) 0.1 s and F) 0.05 s, being in all cases the total time in *on* of 5 s.

Fig. 3) at 44.95, 65.5 and 82.9°2θ are assigned to a cubic phase of α-CoFe alloy (PDF #49-1568). The peaks marked in blue, located at 11.6, 22.9, 34.2, 59.3 and 60.6°2θ, can be assigned to CoFe-LDH, similar structure that those of NiFe//LDH, shown by Hunter et al. [20], and CoFe//LDH (PDF #50-235 card) in which the intercalate anion is $CO_3{}^{2-}$. Therefore, the deposits formed present, over the granular CoFe alloy, oxidized species of Fe and/or Co, formed as a consequence of the local pH variation during electrodeposition and

hydrogen evolution, in a layered structure with, probably, intercalated with Cl$^-$ anion, in excess in the solution. XRD pattern of the deposit obtained for 60 s on GC (Fig. SM3) corroborates the information extracted from Fig. 3. This structure is confirmed by XPS (Fig. 4). The hydroxides structure is constituted by a layered double hydroxide of Co^{2+} and Fe^{3+} (LDH), with chloride inserted in the interlayer.

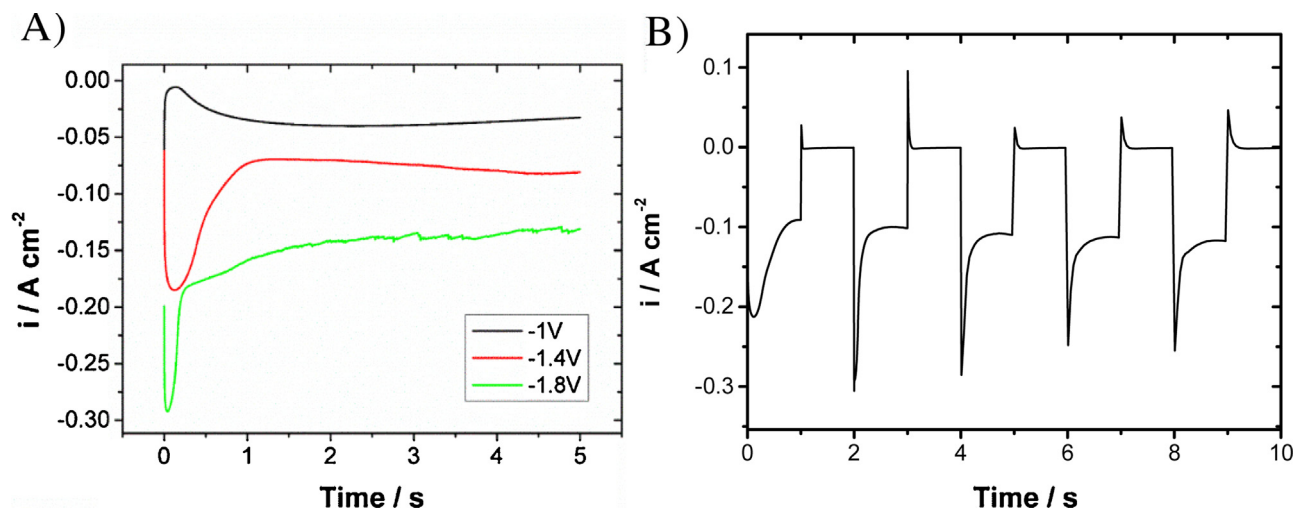**Fig. 2.** i–t curves obtained on glassy carbon at different protocols, A) continous deposition during 5 s at different potentials; B) during 10 s by pulse deposition with 1 s pulse. Electrodeposition bah 100 mM $CoCl_2$ + 100 mM $FeCl_2$ + 500 mM KCl aqueous solution.
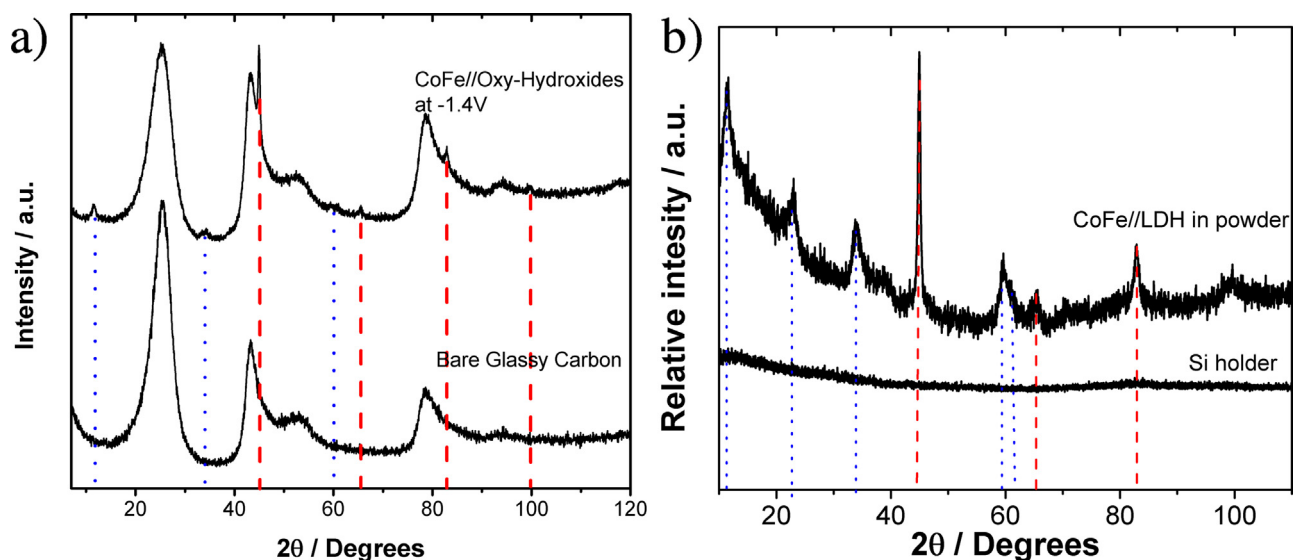

Fig. 3. XRD patterns of deposits obtained at −1.4 V, a) directly on the glassy carbon substrate, and b) in powder form on silicon holder substrate. Dotted line: CoFe//LDH, dashed line: α-CoFe.

The XPS survey spectrum (Fig. 4a) reveals that the CoFe//LDH deposited at −1.4 V is composed by Cl, O, Fe, and Co, while carbon is observed due to the glassy carbon substrate and atmospheric CO_2. The global composition of the electrodeposits was obtained by EDS (more penetrative technique), which reveals a Co:Fe atomic ratio around 1:1, and a chloride content decreasing as the pulse time decreases (from 4% to 0%, See supplementary material Table S1). This global Co:Fe ratio in the deposit agrees with the bath composition and, according to Burke et al. [19], is a good value for the OER. In addition, the proposed method permits obtaining deposits with high contents of iron, which is very interesting in economic aspects. Chlorinated species such as iron hydroxychloride ($Fe_2(OH)_3Cl$) and cobalt hydroxychloride ($Co_2(OH)_3Cl$) may depict similar behavior for chloride incorporation, but the XRD analysis indicates the possible formation of CoFe//LDH with intercalated Cl^-. The hydroxychlorides and LDH with intercalated chloride depict a content of Cl around 20 at.% [20,21], suggesting that in the deposit, a mixture of oxidized species is grown. The high resolution XPS spectra of Co 2p (Fig. 4b) shows two characteristic peaks at 782.1 and 798.2 eV related to Co $2p_{1/2}$ and Co $2p_{3/2}$, respectively. The dif-

ference between the binding energy of Co $2p_{1/2}$ and Co $2p_{3/2}$ is around 16 eV, which is characteristic of $Co(OH)_2$ species, revealing that such species have predominantly the Co^{2+} oxidation state [22]. The small peak at 777.3 eV is related to Co^0 species, which is in agreement with the metallic underlayer mentioned above [23]. The deconvoluted Fe 2p spectra (Fig. 4c) displays two peaks at 712.6 and 725.6 eV related to Fe $2p_{3/2}$ and Fe $2p_{1/2}$, respectively, and a satellite peak of Fe $2p_{3/2}$ at 717.8 eV, which are commonly attributed to Fe^{3+} species [24,25]. This is supported by the FeOOH structure found by Raman (Fig. 5). The deconvoluted spectra of O 1s (Fig. 4d) displays peaks at 528.2, 530.1 and 532.3 eV, which are attributed to O^{2-}, OH^- and O^- ions [26], respectively. The XPS results reveal that a mixture of Fe and Co LDH composes the deposits obtained and a metallic underlayer mainly composed by cobalt are formed at −1.4 V, during the fast deposition process, as expected.

Representative Raman spectra of CoFe//LDH obtained at −1.4 V (Fig. 5A) show bands in the range from 250 to 700 cm^{-1} that are typical of $Co(OH)_2$ (black dashed lines) and of γ-FeOOH (lepidocrocite – red dashed lines) [22,27]. A small band at 682 cm^{-1} (blue dashed line) can be assigned to active A_g mode attributed to a cubic inverse-
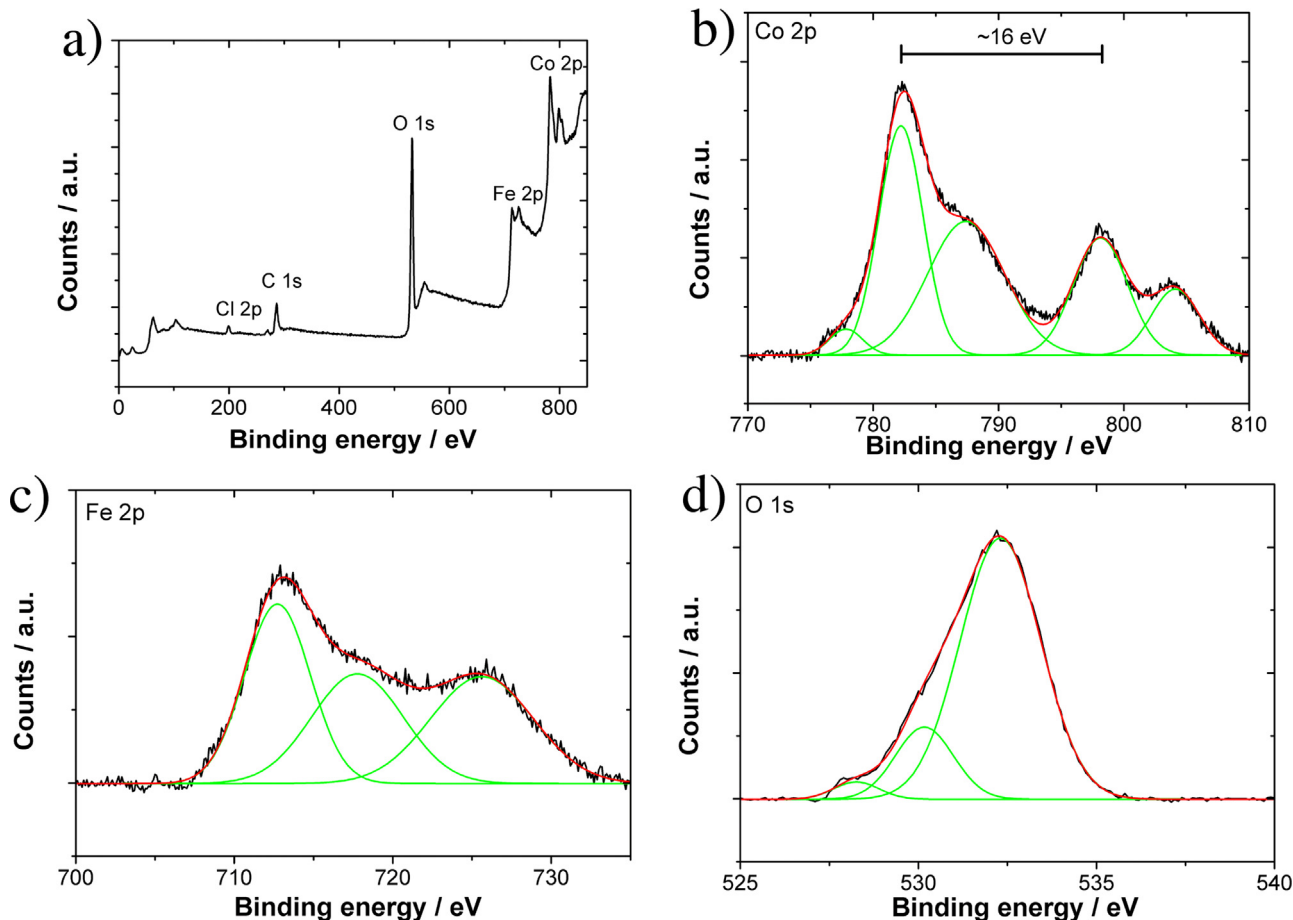
Fig. 4. a) XPS survey spectrum and high resolution spectra for: b) Co 2p, c) Fe 2p and d) O 1s of the deposit obtained at −1.4 V/Ag|AgCl|KCl$_{3M}$ during 5 s.

spinel of mixed CoFe oxides [28] and also to Fe—O—H bending vibration [29]. Other bands at high wavenumbers are shown in Fig. SM4 and can be assigned to the carbon substrate (2920 cm^{-1}) and to the presence of O—H bonds (3520 cm^{-1}) [29,30], which indicate the presence of hydroxides. The band at 523 cm^{-1} is a contribution of the two kinds of hydroxides, which can be associated with a (A_g) symmetric stretching mode of Co(OH)$_2$ and a characteristic band of lepidocrocite. However, the presence of lepidocrocite is detected by the band at 257 cm^{-1} that identifies the γ-FeOOH phase which differs from other phases such as α-FeOOH and δ-FeOOH [27]. The XRD pattern reveals a small peak at 11.9°2θ that could be attributed to β-FeOOH (akaganeite) or to CoFe-LDH which contrasts with the Raman results that evidences the γ-FeOOH phase. The presence of γ-FeOOH is an indicative of the formation of LDH and ledipocrocite on the electrode surface. The attribution of the shoulder band at 595 cm^{-1} is unknown by the authors and will be investigated in further studies. Other bands at high wavenumbers are shown in Fig. SM4 and can be assigned to the carbon substrate (2920 cm^{-1}) and to the presence of O—H bonds (3520 cm^{-1}) [29,30], which indicate the presence of hydroxides (Fig. 5B).

The efficacy of the obtained CoFe//LDH deposits as catalysts for OER has been tested. For this purpose, polarization curves of deposits formed at different potentials were recorded in 1 M NaOH solution, at 5 mV s^{-1}, until the oxygen evolution (Fig. 6). Onset potential, Tafel slopes, and overpotential at 10 mA cm^{-2}, as usual [31,32], were determined for the different obtained deposits (Table 1). In all cases, the behavior of the deposits clearly improved with respect to bare glassy carbon substrates. The overpotential (also the onset potential and Tafel slopes) for the OER improved (decrease) when pulse deposition was used, being the best result

Table 1
Kinetic and catalytic parameters of the CoFe electrodeposits obtained at different pulsed time.

Deposition pulse time/s	Tafel Slope/m V dec^{-1}	Ovepotential/mV at 10 mA cm^{-2}	Onset over-potential/mV
Bare GC	94	447	343
314	62		272
1	50	292	261
0.5	48	286	258
0.25	45	291	264
0.1	44	299	269
0.05	52	303	269

obtained for pulses of 0.5 s. Therefore, the CoFe//LDH samples prepared at −1.4 V with pulsed time of 0.5 s have better catalytic properties for OER, which is justified by the high proportion of hydroxides layer in the deposits and its spongious structure, with a very high active surface. Nevertheless, when duration of the pulses was very low, less proportion of the oxidized layer was formed, with less catalytic effect for OER. The composition of the films obtained by EDS (Table SM1) corroborates the lower content of both oxides and chloride as the pulse time decreases. In this sense, CoFe alloy shows lower catalytic properties for OER than the LDH formed during the electrodeposition. This is also confirmed when the catalytic response to OER of deposits obtained at different potentials, potentiostatic continuous protocol, is compared (Fig. 7). The best effectiveness for the OER is observed for the deposits obtained at −1.4 V, formed by CoFe//LDH. When deposits are formed at less negative deposition potential (−1.0 V), hydrogen evolution is low significant, and the low variation of local pH is not able to induce
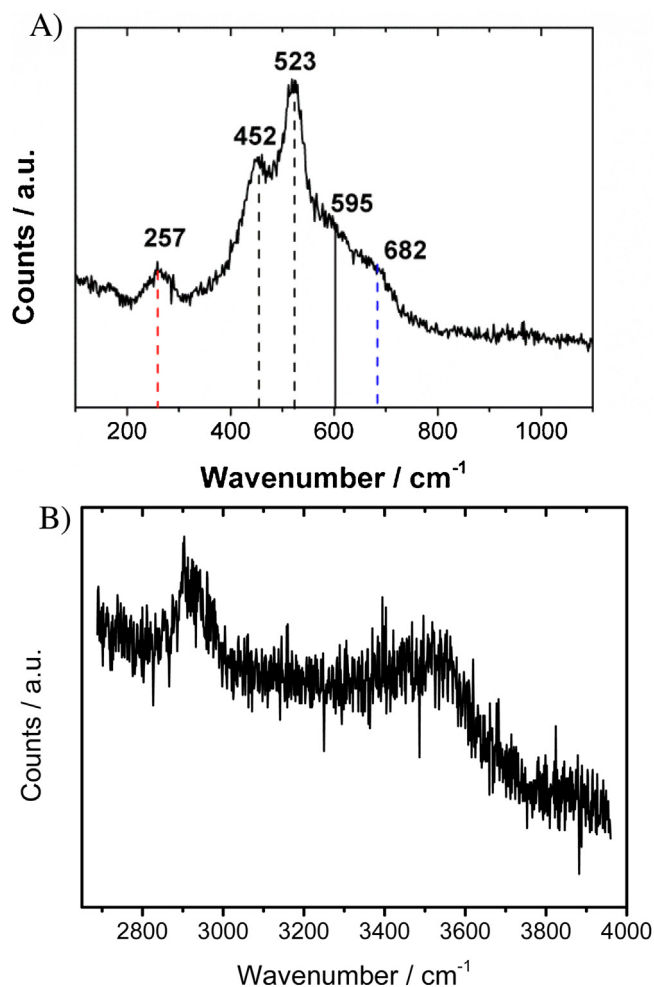
Fig. 5. Raman spectra of the deposit obtained at −1.4 V/Ag|AgCl|KCl$_{3M}$ during 5 s. At A) low and B) high wavelength.

Fig. 7. A) Polarization curves for deposits obtained at different potentials in continuous mode and recorded in 1 M NaOH solution at 5 mV s^{-1}.

significant hydroxides formation. On the other hand, when the deposition potential is excessively negative (−1.8 V), only a layer of low conductive oxidized species is formed. The best conditions for the preparation of the OER catalysts are, then, those than lead to a granular conductive underlayer of CoFe alloy covered with a LDH structure containing hydroxide species with intercalated chloride. For the global process occurring on a hydrous oxide electrode pre-
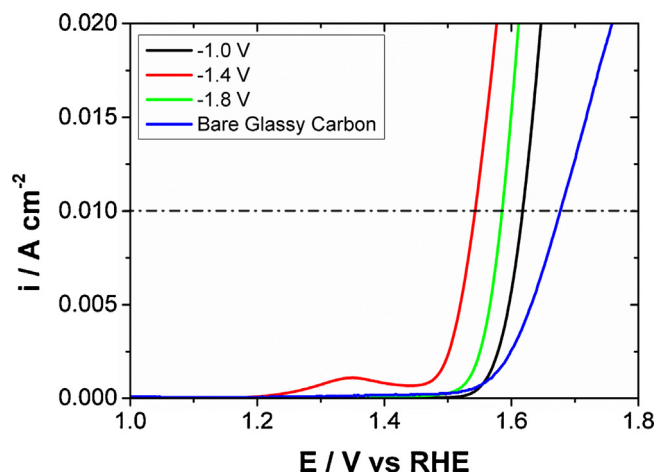
pared at −1.4 V, the Tafel slope can be attributed to the second step, which is the rate-determining step [33].

In order to assure the durability of the catalyst, stability tests were performed, by applying to the deposits a current density of 10 mA cm^{-2} during 5 h. When the deposits obtained in continuous or pulsed conditions were compared (Fig. 8), an overpotential of 313 mV with a slight increase of 66 µV min^{-1} were observed for the deposits obtained in continuous by the deposition protocol, while the deposits prepared by pulse deposition mode with pulses of 0.5 s, show a lower overpotential (298 mV) and excellent stability (increase of only 1.2 nV min^{-1}). This corroborates the excellent performance of the CoFe//LDH deposits obtained at −1.4 V by the pulse deposition procedure as catalysts for OER. In Table 2 the performance of the best deposits obtained in this work with respect to OER is compared with the performance of other catalysts based on transition metals proposed in literature. Our proposal for OER catalysts preparation improves clearly the previous results because not only allows to prepare catalysts with lower overpotential, Tafel slope and onset potential for the reaction, but also implies an easier preparation method, (one-step electrodeposition process in a simple bath) and, moreover, much shorter preparation time(few seconds only).
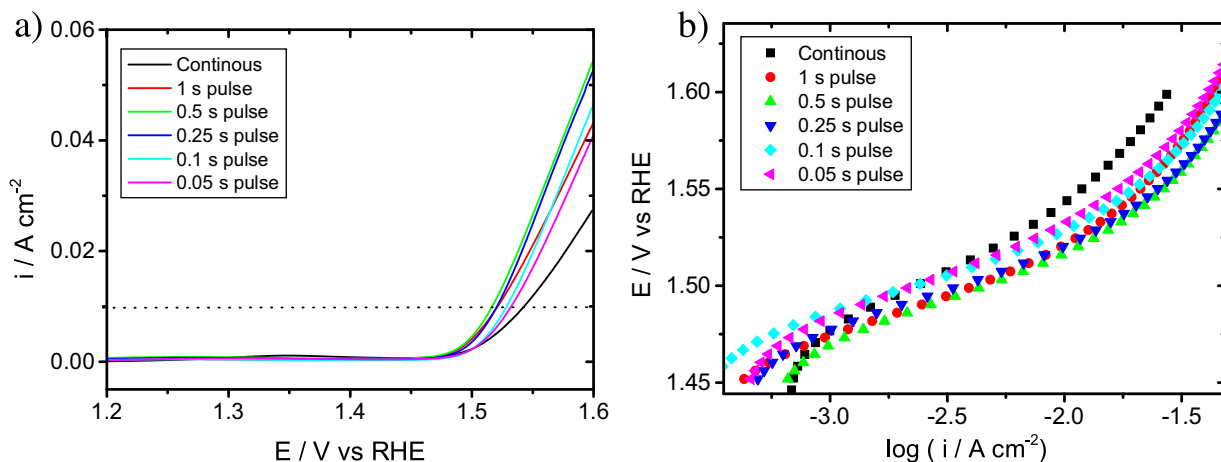

Fig. 6. a) Polarization curves and b) Tafel plot of the deposits obtained at different pulsed times with E$_{on}$ = −1.4V.

Table 2
Comparison of catalytic parameters and experimental conditions of catalysts preparation for OER.

| Material	Overpotential $(10\,mA\,cm^{-2})$/mV	Tafel slope/mV dec^{-1}	Electrolyte	Substrate	Preparation Time	Reference
CoFe//LDH – continuous	314	60	1 M KOH	GC	5 s	This Work
CoFe//LDH – pulsed 0.1	286	48	1 M KOH	CG	10 s (t_{on} = 5 s)	This Work
CoFe35 LDH	351	49	0.1 M KOH	GC	2.5 h	[34]
Co$_x$Fe$_{3-x}$O$_4$	420	53	1 M NaOH	Au and Cu	45 to 150 s	[11]
PI/CNT-Co(OH)$_2$	317	49	KOH	PI/CNT	10 min	[35]
CoFe-LDH	300	83	1 M KOH	NF	48 hours	[36]
Co$_{0.54}$Fe$_{0.46}$OOH	390	47	0.1 M KOH	GC	21–46 h	[32]
CoFeO$_x$	270	36	1 M KOH	NF	2000 s	[37]
Fe-Co composite	283	34	1 M KOH	CFP	30 min	[38]
Co nanoparticles	390	–	0.1 M KOH	GC	1 h	[39]
Co$_3$O$_4$/N-rmGO	310	67	0.1 M KOH	CFP	13 h	[40]
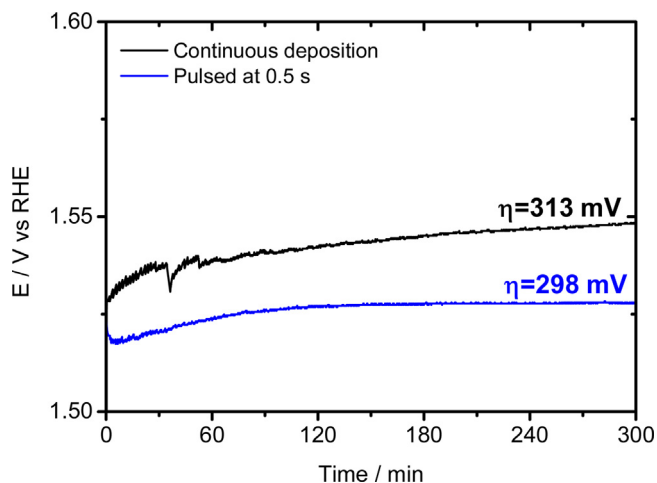
Fig. 8. Stability test obtained by applying $10\,mA\,cm^{-2}$ during 5 h for the deposit obtained at $-1.4\,V/Ag|AgCl|KCl_{3M}$ at constant and pulsed deposition at 0.5 s.

4. Conclusion

In summary, a novel, facile, fast, nitrate-free, and one-step electrosyntehsis has been proposed to directly prepare CoFe thin films covered by layered double hydroxides with enhanced catalytic activity for OER. The Co and Fe oxidized species at the surface of the composite material and the presence of the LDH structure intercalating chloride directly formed over a glassy carbon substrate result in an efficient and cost-effective electrocatalyst for water splitting. The CoFe//LDH prepared at $-1.4\,V$ by continuous deposition and pulsed deposition (0.5 s) shows an overpotential of 314 mV and 286 mV (at $10\,mA\,cm^{-2}$) with a Tafel slope of 62 and 48 mV dec^{-1}, respectively, indicating to be a promising catalyst for OER. The adjustment of the electrosynthesis potential and pulses is fundamental in order to avoid the formation of pure alloy or excessive hydroxides. Furthermore, a new approach to prepare a binder-free electrocatalyst has been developed.

Acknowledgments

Appendix A. Supplementary data

Supplementary material related to this article can be found, in the online version, at doi:https://doi.org/10.1016/j.apsusc.2017.11.042

References

[1] L. Gong, D. Ren, Y. Deng, B.S. Yeo, Efficient and stable evolution of oxygen using pulse-electrodeposited Ir/Ni oxide catalyst in Fe-spiked KOH electrolyte, ACS Appl. Mater. Interfaces 8 (2016) 15985–15990, http://dx.doi.org/10.1021/acsami.6b01888.

[2] M. Gong, Y. Li, H. Wang, Y. Liang, J.Z. Wu, J. Zhou, et al., An advanced Ni-Fe layered double hydroxide electrocatalyst for water oxidation, J. Am. Chem. Soc. 135 (2013) 8452–8455, http://dx.doi.org/10.1021/ja4027715.

[3] R. Chen, G. Sun, C. Yang, L. Zhang, J. Miao, Nanoscale horizons achieving stable and efficient water oxidation by incorporating NiFe layered double hydroxide nanoparticles into aligned carbon nanotubes, Nanoscale Horizons 1 (2016) 156–160, http://dx.doi.org/10.1039/C5NH00082C.

[4] Y. Lee, J. Suntivich, K.J. May, E.E. Perry, Y. Shao-Horn, Synthesis and activities of rutile IrO$_2$ and RuO$_2$ nanoparticles for oxygen evolution in acid and alkaline solutions, J. Phys. Chem. Lett. (2012) 399–404, http://dx.doi.org/10.1021/jz2016507.

[5] I. Roger, M.A. Shipman, M.D. Symes, Earth-abundant catalysts for electrochemical and photoelectrochemical water splitting, Nat. Rev. Chem. 1 (2017) 0003, http://dx.doi.org/10.1038/s41570-016-0003.

[6] P. Cai, Y. Hong, S. Ci, Z. Wen, In situ integration of CoFe alloy nanoparticles with nitrogen-doped carbon nanotubes as advanced bifunctional cathode catalysts for Zn–air batteries, Nanoscale 8 (2016) 20048–20055, http://dx.doi.org/10.1039/C6NR08057J.

[7] P. Cai, S. Ci, E. Zhang, P. Shao, C. Cao, Z. Wen, FeCo alloy nanoparticles confined in carbon layers as high-activity and robust cathode catalyst for Zn-Air battery, Electrochim. Acta 220 (2016) 354–362, http://dx.doi.org/10.1016/j.electacta.2016.10.070.

[8] X. Xiao, C.-T. He, S. Zhao, J. Li, W. Lin, Z. Yuan, et al., A general approach to cobalt-based homobimetallic phosphide ultrathin nanosheets for highly efficient oxygen evolution in alkaline media, Energy Environ. Sci. 10 (2017) 893–899, http://dx.doi.org/10.1039/C6EE03145E.

[9] E. Nurlaela, T. Shinagawa, M. Qureshi, D.S. Dhawale, K. Takanabe, Temperature dependence of electrocatalytic and photocatalytic oxygen evolution reaction rates using NiFe oxide, ACS Catal. 6 (2016) 1713–1722, http://dx.doi.org/10.1021/acscatal.5b02804.

[10] Y. Hou, M.R. Lohe, J. Zhang, S. Liu, X. Zhuang, X. Feng, Vertically oriented cobalt selenide/NiFe layered-double-hydroxide nanosheets supported on exfoliated graphene foil: an efficient 3D electrode for overall water splitting, Energy Environ. Sci. 9 (2016) 478–483, http://dx.doi.org/10.1039/C5EE03440J.

[11] S. Han, S. Liu, S. Yin, L. Chen, Z. He, Electrodeposited Co-doped Fe3O4 thin films as efficient catalysts for the oxygen evolution reaction, Electrochim. Acta 210 (2016) 942–949, http://dx.doi.org/10.1016/j.electacta.2016.05.194.

[12] W. Liu, H. Liu, L. Dang, H. Zhang, X. Wu, B. Yang, et al., Amorphous Cobalt–Iron Hydroxide Nanosheet Electrocatalyst for Efficient Electrochemical and Photo-Electrochemical Oxygen Evolution, 2017, doi:10.1002/adfm.201603904.

[13] X. Lu, C. Zhao, Electrodeposition of hierarchically structured three-dimensional nickel–iron electrodes for efficient oxygen evolution at high current densities, Nat. Commun. 6 (2015) 1–7, http://dx.doi.org/10.1038/ncomms7616.

[14] M. Palomar-Pardavé, B.R. Scharifker, E.M. Arce, M. Romero-Romo, Nucleation and diffusion-controlled growth of electroactive centers: reduction of protons during cobalt electrodeposition, Electrochim. Acta 50 (2005) 4736–4745, http://dx.doi.org/10.1016/j.electacta.2005.03.004.

[15] D. Grujicic, B. Pesic, Electrochemical and AFM study of cobalt nucleation mechanisms on glassy carbon from ammonium sulfate solutions, Electrochim. Acta 49 (2004) 4719–4732, http://dx.doi.org/10.1016/j.electacta.2004.05.028.

[16] J.A. Koza, M. Uhlemann, A. Gebert, L. Schultz, The effect of a magnetic field on the pH value in front of the electrode surface during the electrodeposition of Co, Fe and CoFe alloys, J. Electroanal. Chem. 617 (2008) 194–202, http://dx.doi.org/10.1016/j.jelechem.2008.02.009.

[17] J.A. Koza, M. Uhlemann, A. Gebert, L. Schultz, Nucleation and growth of the electrodeposited iron layers in the presence of an external magnetic field, Electrochim. Acta 53 (2008) 7972–7980, http://dx.doi.org/10.1016/j.electacta.2008.06.011.

[18] L.D. Rafailović, D.M. Minić, H.P. Karnthaler, J. Wosik, T. Trišović, G.E. Nauer, Study of the dendritic growth of Ni–Co alloys electrodeposited on Cu

substrates, J. Electrochem. Soc. 157 (2010) D295–D301, http://dx.doi.org/10.1149/1.3336957.

[19] M.S. Burke, M.G. Kast, L. Trotochaud, A.M. Smith, S.W. Boettcher, Cobalt-iron (oxy)hydroxide oxygen evolution Electrocatalysts: the role of structure and composition on activity, stability, and mechanism, J. Am. Chem. Soc. 137 (2015) 3638–3648, http://dx.doi.org/10.1021/jacs.5b00281.

[20] B.M. Hunter, W. Hieringer, J.R. Winkler, H.B. Gray, A.M. Müller, Effect of interlayer anions on [NiFe]-LDH nanosheet water oxidation activity, Energy Environ. Sci. 9 (2016) 1734–1743, http://dx.doi.org/10.1039/C6EE00377J.

[21] G.D. Park, Y.N. Ko, Y.C. Kang, Electrochemical properties of cobalt hydroxychloride microspheres as a new anode material for Li-ion batteries, Sci. Rep. 4 (2014) 5785, http://dx.doi.org/10.1038/srep05785.

[22] J. Yang, H. Liu, W.N. Martens, R.L. Frost, Synthesis and characterization of cobalt hydroxide, cobalt oxyhydroxide, and cobalt oxide nanodiscs, J. Phys. Chem. C 114 (2010) 111–119, http://dx.doi.org/10.1021/jp908548f.

[23] N. Jiang, B. You, M. Sheng, Y. Sun, Electrodeposited cobalt-phosphorous-derived films as competent bifunctional catalysts for overall water splitting, Angew. Chem.–Int. Ed. 54 (2015) 6251–6254, http://dx.doi.org/10.1002/anie.201501616.

[24] Y.Q. Gao, X.Y. Liu, G.W. Yang, Amorphous mixed-metal hydroxide nanostructures for advanced water oxidation catalysts, Nanoscale 8 (2016) 5015–5023, http://dx.doi.org/10.1039/c5nr08989a.

[25] Y. Mu, F. Jia, Z. Ai, L. Zhang, Iron oxide shell mediated environmental remediation properties of nano zero-valent iron, Environ. Sci. Nano 4 (2017) 27–45, http://dx.doi.org/10.1039/C6EN00398B.

[26] J.-C. Dupin, D. Gonbeau, P. Vinatier, A. Levasseur, Systematic XPS studies of metal oxides, hydroxides and peroxides, Phys. Chem. Chem. Phys. 2 (2000) 1319–1324, http://dx.doi.org/10.1039/a908800h.

[27] D.L.A. de Faria, S. Venâncio Silva, M.T. de Oliveira, Raman microspectroscopy of some iron oxides and oxyhydroxides, J. Raman Spectrosc. 28 (1997) 873–878, http://dx.doi.org/10.1002/(SICI)1097-4555(199711)28:11<873::AID-JRS177>3.0.CO;2-B.

[28] J. Jiang, J. Zhu, R. Ding, Y. Li, F. Wu, J. Liu, et al., Co–Fe layered double hydroxide nanowall array grown from an alloy substrate and its calcined product as a composite anode for lithium-ion batteries, J. Mater. Chem. 21 (2011) 15969, http://dx.doi.org/10.1039/c1jm12670a.

[29] D.S. Dunn, M.B. Bogart, C.S. Brossia, G.A. Cragnolino, Corrosion of iron under alternating wet and dry conditions, Corrosion 56 (2000) 470–481, http://dx.doi.org/10.5006/1.3280551.

[30] L. Bellot-Gurlet, D. Neff, S. Réguer, J. Monnier, M. Saheb, P. Dillmann, Raman studies of corrosion layers formed on archaeological irons in various media, J.

Nano Res. 8 (2009) 147–156, http://dx.doi.org/10.4028/www.scientific.net/JNanoR.8.147.

[31] K.-L. Yan, X. Shang, Z. Li, B. Dong, X. Li, W.-K. Gao, et al., Ternary mixed metal Fe-doped NiCo 2 O 4 nanowires as efficient electrocatalysts for oxygen evolution reaction, Appl. Surf. Sci. (2017), http://dx.doi.org/10.1016/j.apsusc.2017.04.204.

[32] X. Zhang, L. An, J. Yin, P. Xi, Z. Zheng, Y. Du, Effective construction of high-quality iron oxy-hydroxides and co-doped iron oxy-hydroxides nanostructures: towards the promising oxygen evolution reaction application, Sci. Rep. 7 (2017) 43590, http://dx.doi.org/10.1038/srep43590.

[33] R.L. Doyle, I.J. Godwin, M.P. Brandon, M.E. Lyons, Redox and electrochemical water splitting catalytic properties of hydrated metal oxide modified electrodes, Phys. Chem. Chem. Phys. 15 (2013) 13737–13783, http://dx.doi.org/10.1039/c3cp51213d.

[34] F. Yang, K. Sliozberg, I. Sinev, H. Antoni, A. Bähr, K. Ollegott, et al., Synergistic effect of cobalt and iron in layered double hydroxide catalysts for the oxygen evolution reaction, ChemSusChem 10 (2017) 156–165, http://dx.doi.org/10.1002/cssc.201601272.

[35] Y. Jiang, X. Li, T. Wang, C. Wang, Enhanced electrocatalytic oxygen evolution of a-Co(OH)2 nanosheets on carbon nanotube/polyimide film, Nanoscale (2016) 9667–9675, http://dx.doi.org/10.1039/C6NR00614K.

[36] L. Feng, A. Li, Y. Li, J. Liu, L. Wang, L. Huang, et al., A highly active CoFe layered double hydroxide for water splitting, ChemPhysChem 82 (2017) 483–488, http://dx.doi.org/10.1002/cplu.201700005.

[37] C.G. Morales-Guio, L. Liardet, X. Hu, Oxidatively electrodeposited thin-film transition metal (oxy)hydroxides as oxygen evolution catalysts, J. Am. Chem. Soc. 138 (2016) 8946–8957, http://dx.doi.org/10.1021/jacs.6b05196.

[38] W. Liu, K. Du, L. Liu, J. Zhang, Z. Zhu, Y. Shao, et al., One-step electroreductively deposited iron-cobalt composite films as efficient bifunctional electrocatalysts for overall water splitting, Nano Energy (2016) 0–1, http://dx.doi.org/10.1016/j.nanoen.2016.11.047.

[39] L. Wu, Q. Li, C.H. Wu, H. Zhu, A. Mendoza-Garcia, B. Shen, et al., Stable cobalt nanoparticles and their monolayer array as an efficient electrocatalyst for oxygen evolution reaction, J. Am. Chem. Soc. 137 (2015) 7071–7074, http://dx.doi.org/10.1021/jacs.5b04142.

[40] Y. Liang, Y. Li, H. Wang, J. Zhou, J. Wang, T. Regier, et al., Co3O4 nanocrystals on graphene as a synergistic catalyst for oxygen reduction reaction, Nat. Mater. 10 (2011) 780–786, http://dx.doi.org/10.1038/nmat3087.